

# Punctures in a hybrid MR/X-ray-Angiography suite using MR image overlay and stereoscopic x-ray navigation: A study in Phantoms, Animals and a Patient

B. Meyer<sup>1</sup>, D. L. Kraitchman<sup>2</sup>, A. Brost<sup>3</sup>, L. Yatziv<sup>4</sup>, N. Strobel<sup>5</sup>, W. Gilson<sup>6</sup>, J. S. Lewin<sup>2</sup>, and F. K. Wacker<sup>2</sup>

<sup>1</sup>Radiology, Charite, Berlin, Germany, <sup>2</sup>The Russell H. Morgan Department of Radiology and Radiological Science, Johns Hopkins University, Baltimore, MD, United States, <sup>3</sup>Informatics - Pattern Recognition, Universitaet Erlangen, Erlangen, Germany, <sup>4</sup>Siemens Corporate Research, Princeton, NJ, United States, <sup>5</sup>AX Division, Siemens Medical Solutions, Forchheim, Germany, <sup>6</sup>Siemens Corporate Research, Baltimore, MD, United States

## Introduction

Currently, percutaneous punctures for biopsy, drainage and therapy rely on ultrasound and computed tomography guidance. More recently, magnetic resonance guided punctures have been shown to provide accurate targeting. However, these procedures require special non-ferromagnetic devices and are in general more challenging to perform. These challenges have led to the development of robotic and navigation tools that facilitate MR guided punctures without the need for the operator to reach inside the magnet. In this study, a hybrid MR/X-ray-Angiography suite was used for imaging, targeting and navigation. MR imaging was used to identify the target lesions. The actual puncture was then performed in the angiographic C-arm using stereoscopic navigation. The roadmap information provided by MR imaging was used as an overlay, to facilitate the “MR-guided” puncture. The purpose of this study was to test the feasibility and accuracy of the stereoscopic X-ray based MR overlay navigation in a hybrid MR/X-ray-Angiography suite for percutaneous punctures in phantoms, animals and a patient.

## Method

The experiments were performed in a hybrid MR/X-ray-Angiography suite equipped with a 1.5 Tesla closed bore magnet system (Magnetom Espree, Siemens Medical Solutions, Erlangen, Germany) and an angiography flat detector C-arm (Axiom-Artis dFA, Siemens Medical Solutions, Forchheim, Germany). The biopsy phantoms consisted of plastic buckets filled with gelatin. To mimic lesions within the phantom, 20 plastic rings not visible under fluoroscopy with a 10 mm inner diameter and 1 mm height were embedded in the gel. The rings were placed at different spatial locations and levels. A 20cm long 18-gauge needle was used for all punctures. In vivo animal experiments were conducted under general anesthesia on two pigs using an approved institutional animal care and use committee protocol. In one patient, the MR overlay was used in combination with the navigation device for a targeted puncture under local anesthesia.

The prototype navigation software requires three steps. First, MR images are acquired using an axial gradient echo sequence (FLASH3D, TR,TE: 9, 5 ms; 25° flip angle; 1mm slice thickness). Then, the phantoms/animals were transferred to the angiography C-arm and a 8s C-arm CT (DynACT®, Siemens Medical Solutions, Forchheim, Germany) was performed. The 3D data sets were sent to the navigation workstation using a LAN Ethernet connection and MRI and CACT data sets were co-registered using commercial fusion software with the CACT providing the spatial information and the MR providing the soft tissue contrast to detect the lesions. For puncture guidance, stereo-fluoroscopic images were used to detect and interactively guide the needle towards the targets. The needle path was graphically enhanced with a thin virtual cylinder and rings that marked the entry point and the target. 20 phantom punctures and 10 punctures in the animals were completed. Prior to every experiment, the needle path was planned based on multiplanar images of the 3D datasets and visualized on the fluoroscopic images. Upon completion of the ring punctures, gadolinium doped gel droplets (phantoms) and wire fragments (animals) were inserted through the needle to mark the needle tip position. MR control scans were acquired in order to measure the distance of the needle tip/marker to the target for calculation of the Euclidian distance. In the patient procedure, Gd-EOB-DTPA (Primovist®, Bayer-Schering AG, Berlin) enhanced MR images were acquired one day prior to the puncture. During the procedure, the MR images were fused with the C-arm CT and used for targeting. Success was determined by inserting a guide wire into the leaking bile duct.

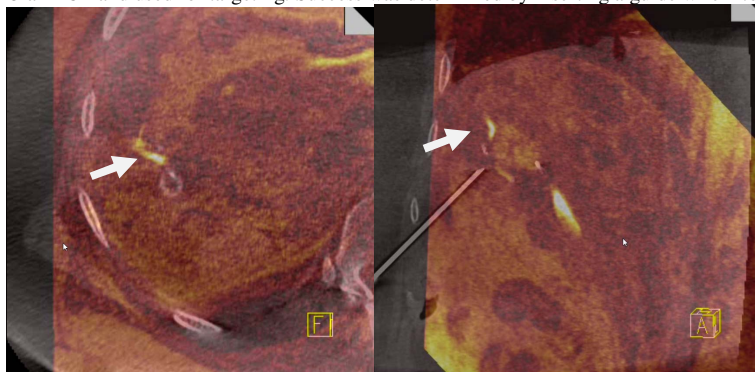


**Fig. 1:** Screenshot of the fused MR image (red overlay) and the CACT dataset before (axial, a) and after (coronal oblique, b) the puncture. The contrast extravasation (arrow) can be appreciated.

## Results

In the ring phantom experiments, the radiologists successfully placed the tip of the needle inside the targets in all twenty 10-mm-diameter rings. Targeting was performed solely based on the information contained in the MR images. The total error (distance from the centre of the plastic ring (target) to the position of the gadolinium droplet) was  $8.58 \text{ mm} \pm 2.84 \text{ mm}$ . In the animal procedures, visualization of the needle trajectory in both, the fluoroscopic and the MR images provided abundant information and guidance, leading to a straightforward puncture whether requiring a single or double angulation of the puncture path. The punctures in pigs were successful in all 10 cases. The total error as defined above was  $7.72 \text{ mm} \pm 2.41 \text{ mm}$ . The operator error (distance from the target point to the final needle position calculated based on stereoscopic location of the needle tip/marker) in the animal procedures was  $5.00 \text{ mm} \pm 2.87 \text{ mm}$  whereas the system error (distance from the final needle position calculated from two fluoroscopic images to that in control CACT) was  $4.23 \text{ mm} \pm 2.34 \text{ mm}$ . In the patient, the bile leak was successfully punctured followed by insertion of a guidewire and subsequent closure of the leak using embolization coils and glue.

## Discussion

The puncture technique presented, which combines spatial information provided by C-arm CT with soft tissue contrast provided by MR imaging, has proven to effectively facilitate image-guided punctures in phantoms, animals and one patient. MR images acquired before the procedures are co-registered using C-arm CT. This provides an elegant means to perform percutaneous interventions in a combined MR/X-ray-Angiography suite (XMR suite). The MR images provide superb soft tissue information and the angiographic C-arm provides good patient access, helps to avoid the need to use MR compatible devices and facilitates excellent follow up imaging for procedures such as occlusion of a bile duct, as presented in our patient. As shown with this case, a hybrid system is not mandatory. Instead, a MR exam was performed one day prior to the procedure in a standard 1.5 T closed bore MR scanner with delayed imaging after using a contrast agent that is excreted through the bile. This allowed clear delineation of the bile leak and facilitated successful occlusion of the leak.

The overall accuracy of the X-ray based navigation in combination with MR-image overlay suggests its safe use. It is extremely beneficial in complicated cases that require special imaging techniques on the MR side to visualize targets that are otherwise not visible. It might also be helpful for more complex procedures that require double-oblique puncture trajectories or positioning of multiple needles/applicators or punctures of multiple lesions.



**Fig. 2:** Screenshot acquired during needle guidance in a pig. Upper row shows fluoroscopy with navigation overlay and needle, lower row shows MR images with needle path (blue/yellow line) and target (blue dot).